

Neutrino flares of radio blazars observed from TeV to PeV

Alisa Suray¹★ and Sergey Troitsky^{2,1}

¹*Physics Department, Lomonosov Moscow State University, 1-2 Leninskie Gory, Moscow 119991, Russia*

²*Institute for Nuclear Research of the Russian Academy of Sciences, 60th October Anniversary prospect 7a, 117312 Moscow, Russia*

Submitted to MNRAS Letters on June 29, 2023. Revised on August 30, 2023. Accepted on September 20, 2023

ABSTRACT

Radio blazars have been linked both to individual high-energy neutrino events and to excesses in likelihood sky maps constructed from lower-energy neutrino data. However, the exact mechanism by which neutrinos are produced in these sources is still unknown. Here, we demonstrate that IceCube neutrinos with energies over 200 TeV, which were previously associated with bright radio blazars, are significantly more likely to be accompanied by flares of lower-energy events, compared to those lacking blazar counterparts. The parsec-scale core radio flux density of blazars, positioned within the error regions of energetic events, is strongly correlated with the likelihood of a day-scale lower-energy neutrino flare in directional and temporal coincidence with the high-energy event, reported by IceCube. The probability of a chance correlation is 3.6×10^{-4} . This confirms the neutrino-blazar connection in a new and independent way, and provides valuable clues to understanding the origin of astrophysical neutrinos.

Key words: neutrinos – galaxies: active – galaxies: jets – quasars: general – radio continuum: galaxies

1 INTRODUCTION

High-energy neutrino sky is presently under active investigation, thanks to new data coming from the IceCube (Aartsen et al. 2017), ANTARES (Ageron et al. 2011), Baikal-GVD (Averorin et al. 2022) and KM3NeT (Adrián-Martínez et al. 2016) observatories. The presence of extraterrestrial neutrinos is well established by different experiments (Aartsen et al. 2013; Abbasi et al. 2021; Fusco & Versari 2019; Allakhverdyan et al. 2023), while their origin is a matter of intense discussions, see e.g. Mészáros (2017); Troitsky (2022) for reviews. The neutrino sky is diverse: while a part of events probably originate in our Galaxy (Kovalev et al. 2022; Albert et al. 2022; ?), others have been associated with extragalactic sources, (e.g. Aartsen et al. 2018b; Giommi et al. 2020; Plavin et al. 2020; Buson et al. 2022; Abbasi et al. 2022b, etc.). Evidence is growing that blazars, which are active galactic nuclei with relativistic jets pointing to the observer (Urry & Padovani 1995), are responsible for a significant part of the high-energy astrophysical neutrino flux. Some of the results refer to individual sources like TXS 0506+056 (Aartsen et al. 2018b,a; Allakhverdyan et al. 2022) or others (Kadler et al. 2016; Rodrigues et al. 2021; Sahakyan et al. 2023), but the most compelling evidence comes from statistical analyses of blazar populations versus neutrino data sets (Plavin et al. 2020, 2021, 2023b; Giommi et al. 2020; Hovatta et al. 2021; Kun et al. 2022; Buson et al. 2022, 2023, etc.).

High-energy neutrino telescopes work in a wide energy band, TeVs to PeVs. Some of previous studies considered highest-energy ($E \gtrsim 200$ TeV) events, selected individually as most probable candidates for astrophysical neutrinos. Other studies used entire data sets, dominated by lower-energy, \sim TeV, events, most of which are caused by muons and neutrinos originating in the terrestrial atmosphere. Statistically significant associations with blazars have been reported

both for the most energetic events (Giommi et al. 2020; Plavin et al. 2020, 2023b) and for excesses in the sky maps built from entire, mostly lower-energy data sets (Plavin et al. 2021; Buson et al. 2022, 2023). This is remarkable since the efficient production of \sim TeV and of $\sim 10^2$ TeV neutrinos requires different conditions in the source, see Sec. 4.3. Because of the statistical nature of the most significant neutrino-blazar links, it was unclear if neutrinos of all energies from TeV to PeV are produced in the same class of sources, or in distinct blazar populations. In the former case, the question would arise whether high- and lower-energy neutrinos are produced simultaneously. The present work addresses these questions and searches for correlations of individual high-energy IceCube events, associated with blazars, with coincident flares of lower-energy neutrinos.

In the rest of the Letter, we discuss the data we use (Sec. 2), addressing separately the blazar sample (Sec. 2.3), high-energy neutrinos (Sec. 2.1) and lower-energy neutrino flares (Sec. 2.2). In Sec. 3, we perform the statistical analysis and present its results. We discuss the results and their implications in Sec. 4. In particular, Sec. 4.1 stresses the importance of the selection of events associated with radio blazars for the result; Sec. 4.2 discusses the potential impact of different IceCube event reconstructions on the blazar-related results. Implications of our results for modelling neutrino production in blazars are discussed in Sec. 4.3. We briefly conclude in Sec. 5.

2 DATA

The most direct observational feature of a blazar is its Doppler-boosted radiation from a spatially compact region, indicating a relativistic jet viewed at the angle of a few degrees. Localisation of the emission to parsec-scale cores of cosmologically distance sources is possible only with very-long-baseline interferometry (VLBI) in the radio band, due to its superb angular resolution. VLBI observations are an efficient tool to select blazars (e.g. Blandford et al. 2019),

★ Corresponding author; e-mail: surai.ai21@physics.msu.ru

and a sample of VLBI-selected radio blazars was used to establish, in a statistical way, associations of these sources both with highest-energy (Plavin et al. 2020, 2023b) and lower-energy (Plavin et al. 2021) neutrinos. In the present work, we use the same samples of energetic neutrinos and of radio blazars from Plavin et al. (2023b), supplemented by recently published results of IceCube searches for associated lower-energy flares.

2.1 IceCube high-energy events

Quality cuts for the highest-energy neutrino sample were fixed by Plavin et al. (2020), motivated by requirements of good reconstruction accuracy and of high ratio of the astrophysical signal to the atmospheric background. The cuts select, from event lists published by IceCube, muon tracks with expected progenitor neutrino energy $E_\nu > 200$ TeV and the solid angle enclosed by the 90% CL directional uncertainty contour in the sky $\Omega_{90\%} < 10$ deg². The same, up to addition of more recent events satisfying the same selection criteria, sample was used in a number of subsequent studies (Hovatta et al. 2021; Plavin et al. 2023b,a; Kovalev et al. 2022). Here, we start with the sample of 71 events (Plavin et al. 2023b) supplemented by two recent IceCube alerts issued later (IceCube Collaboration 2022f,h) and passing the same selection cuts. We have to remove 12 events for which no flare data, discussed in Sec. 2.2, are available (in particular, 10 of them were registered before May 2011). Finally, we remove one event for which Abbasi et al. (2023a) reported a coincident IceTop signal, strongly suggesting that this event was atmospheric. The list of 60 events in the final high-energy sample is presented in Supplementary Information I. We recall that about 1/3 of these events are still expected to be of the atmospheric origin (Plavin et al. 2020; Kovalev et al. 2022), but there is no direct way to identify, which ones. In what follows, we call all these 60 events “HE neutrinos” for brevity, though some of them may be caused by atmospheric muons and not neutrinos.

2.2 IceCube lower-energy flares

For each of the public high-energy neutrino alert, IceCube distributes also the information about accompanying lower-energy neutrinos. For archival events between May 2011 and December 2020, this information was collected and published by Abbasi et al. (2022a). For events of 2021–2022, we use the data from GCN circulars (IceCube Collaboration 2021a,b,c, 2022a,b,c,d,e,g,i).

These publications present high-level data for each energetic event, which include the p-value p , measuring the probability that energies and arrival directions of other neutrinos, detected within a certain time window $\pm T$ around the HE neutrino arrival moment, are consistent with the background. Details of the calculation of p are presented by Abbasi et al. (2022a). In our analysis, we use $L \equiv -\log_{10} p$ as a convenient variable (our statistical procedure is not sensitive to any monotonic redefinition of the observable) and call it “likelihood of a flare” for brevity. Of two values of T for which p is reported, 500 s and 1 day, we choose the latter because longer flare durations are suggested by multimessenger observations (Aartsen et al. 2018b; Plavin et al. 2020; Hovatta et al. 2021; Allakhverdyan et al. 2022). Note that for any individual event, the accompanying flare is not significant, with the highest $L = 1.52$, corresponding to a 2.2σ excess.

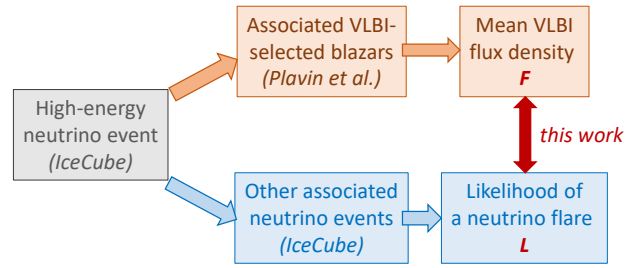


Figure 1. Scheme of the analysis of a high-energy event.

2.3 Radio blazars

Following previous works, we use a complete full-sky flux-density limited sample of blazars selected from the Radio Fundamental Catalog¹ (RFC) by requiring the 8-GHz VLBI average flux density to exceed 0.15 Jy. The RFC sample was compiled from dedicated observations by Beasley et al. (2002); Fomalont et al. (2003); Petrov et al. (2005, 2006, 2008, 2009, 2011a,b, 2019); Petrov (2011, 2012, 2013, 2021); Kovalev et al. (2007); Pushkarev & Kovalev (2012); Piner et al. (2012); Schinzel et al. (2015); Gordon et al. (2016); Shu et al. (2017). The isotropy of the sample of potential sources is important when other, anisotropic astrophysical contributions to the total neutrino flux may be present (Kovalev et al. 2022), e.g. the Galactic one. In the present work, this source sample is used to associate radio blazars with simulated neutrino events at the stage of Monte-Carlo estimation of the statistical significance (Sec. 3) and to search for blazar counterparts of two most recent HE neutrinos, see Sec. 2.1. For the rest of events, counterparts from the same RFC 2022b catalog were determined by Plavin et al. (2023b).

3 ANALYSIS AND RESULTS

We address a question, whether blazar-associated HE neutrino events are accompanied by lower-energy neutrino flares. To this end, we obtain, for each HE neutrino, two quantities: one is related to the probability of an association with a blazar, another measures the probability of a neutrino flare. Then the correlation between these two quantities is searched for by standard statistical methods. To estimate how often this or stronger correlation occurs by chance, we use Monte-Carlo simulations.

For an individual HE neutrino, we use the flare likelihood L , published by IceCube and discussed in Sec. 2.2, as the measure of the probability of an associated neutrino flare. To quantify associations with blazars, we follow Plavin et al. (2020, 2023b) and use the mean 8-GHz VLBI flux density F of blazars from the RFC complete, $F > 0.15$ Jy, sample, associated with the events. If more than one blazar is associated with a HE neutrino, F is taken to be equal to their mean flux, while $F = 0$ is set if no associated blazars are present. We use the same procedure for association as determined by Plavin et al. (2020, 2023b), and recollect all the details of this procedure in Supplementary Information II for reference. Therefore, both quantities, L and F , are determined in previous works, see Fig. 1.

¹ http://astrogeo.org/sol/rfc/rfc_2022b/. Note that we use the RFC 2022b version for full consistency with Plavin et al. (2023b), though a newer version is available.

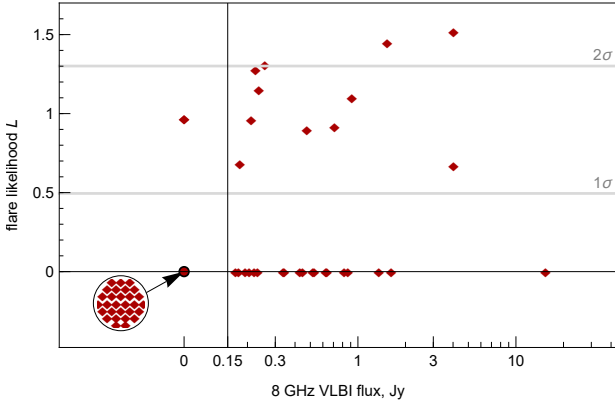


Figure 2. The likelihood L of a lower-energy neutrino flare coincident in time and direction with a high-energy event versus the mean logarithmic 8-GHz VLBI flux density F of blazars associated with the same event. The vertical line indicates the 0.15 Jy flux-density threshold of the sample. Zero flux means no associated blazars, $L = 0$ means no neutrino flare. The circular inset illustrates 29 HE events without associated blazars and neutrino flares. Of 12 events with neutrino flares, 11 are associated with blazars (92%), while only 19 of 48 (40%) of events without flares have blazar counterparts.

We now have two sets, $\{F_i\}$ and $\{L_i\}$, where $i = 1, \dots, 60$ enumerates HE neutrinos. The values of F_i and L_i are collected in Table 2 in Supplementary Information I and presented graphically in Fig. 2. We want to test the null hypothesis that the association of HE neutrinos with radio blazars is unrelated to the low-energy neutrino flares, that is the sets $\{F_i\}$ and $\{L_i\}$ are uncorrelated. To do this, we introduce test statistics which measure the correlation. We then perform Monte-Carlo simulations to see how strong the correlation is.

The relation between the value of $L > 0$ and properties of the possible neutrino flare is unknown, but $L = 0$ corresponds to the absence of accompanying low-energy neutrinos. This motivates the simplest statistics equal to the ratio of mean flux densities of blazars associated with HE neutrinos with $L \neq 0$ to those with $L = 0$, the flux ratio statistics f . We also consider two more common test statistics for correlations between two sets of numbers, the Spearman rank statistics ρ and the Kendall rank correlation coefficient τ . For reference, we collect explicit definitions of f , ρ and τ in Supplementary Information III.

Though some expressions exist which relate values of ρ or τ to the probability of chance correlations, they require certain assumptions about the distribution of uncorrelated values. Therefore we do not use these relations and perform Monte-Carlo simulations to assess the significance of correlations. We simulate artificial HE neutrino sets by assigning random right ascensions to real HE events, keeping declinations, shapes and sizes of error regions, and values of L unchanged. This approach is justified because the sensitivity of IceCube depends on the zenith angle only; any potential dependence on the azimuthal angle related to the detector geometry is washed out by the Earth’s rotation. Scrambling of right ascensions is the standard way to randomize arrival directions in IceCube anisotropy studies (e.g., Abbasi et al. 2023b).

For each artificial set of 60 HE neutrinos, we find associated blazars in the same way it was done for the real data, find the values of F and calculate the same test statistics. We repeat the simulations 10^5 times. The probability of chance correlation is given by the fraction of simulated sets with the same or larger value of the test statistics as obtained for the real data. The results are presented in Table 1.

Test statistics	Observed value	Chance probability
f	2.202	3.0×10^{-4}
ρ	0.419	3.6×10^{-4}
τ	0.363	3.5×10^{-4}

Table 1. Results for three test statistics (see the text for details).

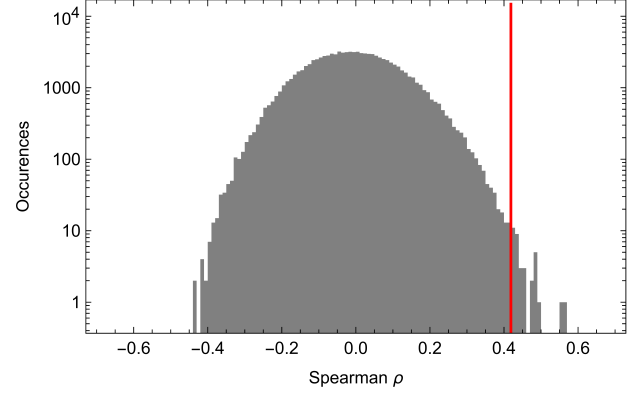


Figure 3. Distribution of Spearman rank test statistics ρ for 10^5 randomized data sets (gray histogram) and the value of ρ_0 for the real data (vertical red line). Only 36 of 10^5 simulated sets have $\rho \geq \rho_0$.

We see that all three tests give similarly low chance probabilities of correlations and conclude that the HE neutrinos associated with radio blazars are significantly more likely accompanied by lower-energy neutrino flares, compared to HE neutrinos lacking blazar counterparts. To be conservative with respect to the three trials (f , ρ , τ), we choose to report the highest chance probability (the lowest significance) as our final result. This is given by the Spearman rank test and corresponds to the equivalent Gaussian significance of 3.6σ . The distribution of simulated values of ρ is presented in Fig. 3. Note that the distribution is slightly asymmetric, which confirms the need of Monte-Carlo simulations to assess the strength of correlations. Similar plots for f and τ are presented in Supplementary Information III.

4 DISCUSSION

4.1 Blazar-associated alerts versus all alerts

In a dedicated study, Abbasi et al. (2022a) addressed a similar question, whether high-energy events are accompanied by lower-energy neutrino flares. They considered all events from the catalog by Abbasi et al. (2023a) and found that the distribution of L for all events is consistent with that expected for random coincidences. We cannot test this result for our sample of 60 events, selected in a different way, because this would require unpublished information. However, we demonstrate that a significant correlation exists between L and the VLBI flux density of associated blazars. This suggests that the association with blazars changes the situation drastically. Among other implications, this gives a strong independent support to the original association (Plavin et al. 2020, 2023b) of HE neutrinos with radio blazars.

Let us estimate roughly the fraction of HE neutrinos coming from radio blazars. The events without a blazar association, or those randomly coincident with blazars, are not expected to correlate with

short-time neutrino flares. About 1/3 of the HE neutrinos in the sample, that is ~ 20 of 60, are atmospheric (Plavin et al. 2023b). Of the ~ 40 remaining astrophysical events, $(28 \pm 9)\%$, that is $\sim (11 \pm 4)$, are expected to have a Galactic origin (Kovalev et al. 2022). The original work by Plavin et al. (2020) estimated the fraction of HE neutrinos physically associated with blazars from the RFC complete sample as $\sim 10/35 \approx 28.5\%$. Plavin et al. (2021) estimated that $\sim 25\%$ of lower-energy neutrinos come from radio bright blazars from the same sample. This is in formal agreement with the 90% CL upper bound by Zhou et al. (2021), $\leq 30\%$, though both estimates were obtained in different frameworks and have their own systematics. Altogether, we expect that ~ 11 HE neutrinos out of 60 are related to blazars from the catalog we analyze. This matches the actual numbers: 12 HE events out of 60 have nonzero flare likelihood L , 11 of which have blazar counterparts. Given the small statistics and large fluctuations, one generally does not expect that exact coincidence of numbers, which however demonstrates the overall consistency of estimates.

Note that the correlation we observe is not dominated by any single source. In particular, this relates to TXS 0506+056, established as a neutrino source independently of, and before, the radio-blazar statistical studies. Contrary, the event of 2017-09-22, associated with this blazar, was not accompanied by a *simultaneous* low-energy neutrino flare. The largest contribution to the correlation we find here comes from PKS 1731–038, associated with two HE neutrinos, both accompanied by lower-energy flares. It was claimed as a probable neutrino source in the first study of radio blazars and HE neutrinos by Plavin et al. (2020), based on the event of 2011-09-30. Subsequently, the second HE neutrino arrived from its direction on 2022-02-05 (?Plavin et al. 2023b). Since it was claimed as a neutrino source in the radio-blazar analysis, and not elsewhere, dropping it from the sample would not be justified. However, we checked that even without the two events associated with PKS 1731–038, our result remains pronounced (3.0σ).

PKS 1731–038 is among the brightest radio blazars in the sky and the only blazar associated with two HE neutrinos in the sample we use. It also dominates the correlation between HE neutrinos and hard X-ray blazars reported by Plavin et al. (2023a). The present study further motivates this individual association.

Due to a statistical nature of the study, one cannot be sure that all of the corresponding blazars are the neutrino sources. The remaining part of extragalactic HE neutrinos may include events coming from blazars beyond the completeness limit of the RFC catalog or from other extragalactic sources like Seyfert galaxies (Abbasi et al. 2022b; Neronov et al. 2023), tidal disruption events (Stein et al. 2021; Reusch et al. 2022), etc.

4.2 Radio-blazar associations in various IceCube reconstructions

Arrival directions of individual neutrinos differ between various published IceCube data sets, indicating the presence of systematic uncertainties in reconstruction (see e.g. Lagunas et al. 2021; Troitsky 2022, and references therein). This is expected given the lack of precise knowledge of ice properties through the km^3 detector volume. In addition, the energies of neutrinos detected by muon tracks, used in our sample, are determined with huge statistical uncertainties, reaching an order of magnitude, see e.g. Aartsen et al. (2018b). Previous studies indicated that blazar associations, found with the help of published IceCube data, may become less pronounced when data obtained in a different reconstruction are used. For instance, the IceCube 7-year sky map (IceCube Collaboration 2020) was used to establish neutrino-blazar associations (Plavin et al. 2021; Buson

et al. 2022), but the 10-year public event catalog (IceCube Collaboration et al. 2021) did not reveal a significant signal (Zhou et al. 2021; though the results of the two analyses do not contradict to each other, Plavin et al. 2022). At energies above 200 TeV, the sample used by Plavin et al. (2023b) (and here) collected event details as they were originally published, and demonstrated significant correlations with radio blazars, but in a similar analysis by Abbasi et al. (2023b), based on recently reprocessed IceCube data (Abbasi et al. 2023a), the effect was found to be much weaker. We repeated our present analysis with the catalog of Abbasi et al. (2023a) and confirmed that the radio-blazar correlation is not pronounced in this case. Consequently, the correlation of blazar-associated energetic events with lower-energy neutrino flares does not show up for the Abbasi et al. (2023a) alert-like event list.

Understanding the reasons for the discrepancies would require a detailed comparison of the data sets and reconstruction procedures, hardly possible outside the IceCube collaboration. Associations of $E > 200$ TeV neutrinos with VLBI-selected blazars, found by Plavin et al. (2020), strengthened (from 3.1σ to 3.6σ) with the addition of the new data (Plavin et al. 2023b), and our present study adds confidence to the origin of a significant part of HE neutrinos in radio blazars (Plavin et al. 2020). One possible reason for weakening the neutrino-blazar signal in the reconstruction of Abbasi et al. (2023a) may be related to significant changes in the estimated energies of events. This may or may not be related to the extensive use of machine learning in newer reconstructions (Abbasi et al. 2023a), which reduces statistical uncertainties but relies heavily on the simulated training sets, for which certain ice properties should be assumed. Future studies with new liquid-water detectors, Baikal-GVD (Averorin et al. 2022) and KM3NeT (Adrián-Martínez et al. 2016), are expected to shed light on these issues.

4.3 Implications for neutrino production mechanisms

Theoretical interpretation of the observational results of the present work will be addressed elsewhere, but some general implications should be mentioned.

Firstly, our result implies that the same blazars, which produce neutrinos of very high, $E > 200$ TeV, energies, are capable to produce simultaneously lower-energy neutrinos. This is nontrivial, because in blazars, neutrinos are expected to be produced in proton-photon collisions (e.g. Böttcher 2019), and the cross section of this process is dominated by the Δ^+ resonance peak. This means that for efficient production of neutrinos, say, of ~ 10 TeV and of ~ 300 TeV, one needs to have target photons with energies 30 times different (see e.g. Plavin et al. 2023a, for discussion and more references). Therefore, narrow thermal spectra of target photons are disfavoured. Production of lower-energy neutrinos requires target photons of proportionally higher energies, reaching the hard X-ray band. These hard X rays, probably Doppler-boosted, are indeed observed from the blazars associated with $E > 200$ TeV events (Plavin et al. 2023a), in agreement with the present study. This reasoning does not apply to exotic proton-proton mechanisms (Neronov & Semikoz 2021) which however explain only sub-PeV neutrinos from blazars and do not address lower energies. More detailed studies of yet unpublished and future data would help to better understand the neutrino spectra of blazars and to constrain the neutrino production mechanisms.

Secondly, the timescale of the flares we studied, determined by the availability of data, was very short, ± 1 day. An excess of the neutrino flux at longer intervals around the arrival of HE neutrinos, not studied by Abbasi et al. (2022a) but covering this 2-day interval, is not excluded. In fact, various observational studies suggest these

longer intervals for blazar neutrino flares (Aartsen et al. 2018a; Plavin et al. 2020; Hovatta et al. 2021). This matches the expectations of models in which relevant proton-photon interactions take place at parsec-scale distances from the central black hole, and the target photons have Compton origin (Plavin et al. 2021; Kalashev et al. 2022). Studies of longer neutrino flares are thus welcome. However, even day-scale neutrino flares might be explained in a two-zone model by Kalashev et al. (2022), because the relevant variability may be inherited from the proton acceleration mechanism, working close to the black hole.

5 CONCLUSIONS

Our study demonstrates that energetic neutrino events coming from radio blazars are accompanied by simultaneous day-scale lower-energy neutrino flares from the same directions. The statistical significance of the correlation exceeds 3.6σ (Gaussian equivalent). Contrary, no significant correlation were found for all events, without a selection by a blazar association. This means that neutrinos of energies from a few TeV to several hundred TeV are jointly produced in radio blazars. This result adds more confidence to previously established association of radio blazars and neutrinos, confirming that about 25% of the high-energy astrophysical neutrino flux originate from the VLBI-selected blazars. In the frameworks of the baseline proton-photon mechanism, our observation suggests the presence of a wide spectrum of target photons in the neutrino production zone. Future high-quality data from neutrino telescopes will help to understand the mechanism of neutrino production in blazars.

ACKNOWLEDGEMENTS

We thank Alexander Plavin and Grigory Rubtsov for helpful discussions of the statistical analysis and of implications of this work. We are indebted to Yuri Kovalev and to the anonymous reviewer for careful reading of the manuscript and for useful comments.

DATA AVAILABILITY

The analysis is entirely based on published data, referenced in the text.

REFERENCES

Aartsen M., et al., 2013, *Science*, **342**, 1242856
Aartsen M. G., et al., 2017, *Journal of Instrumentation*, **12**, P03012
Aartsen M. G., et al., 2018a, *Science*, **361**, 147
Aartsen M. G., et al., 2018b, *Science*, **361**, eaat1378
Abbasi R. U., et al., 2021, *Phys. Rev. D*, **104**, 022002
Abbasi R., et al., 2022a, *arXiv e-prints*, p. [arXiv:2210.04930](https://arxiv.org/abs/2210.04930)
Abbasi R., et al., 2022b, *Science*, **378**, 538
Abbasi R., et al., 2023a, *arXiv e-prints*, p. [arXiv:2304.01174](https://arxiv.org/abs/2304.01174)
Abbasi R., et al., 2023b, *arXiv e-prints*, p. [arXiv:2304.12675](https://arxiv.org/abs/2304.12675)
Adrián-Martínez S., et al., 2016, *Journal of Physics G Nuclear Physics*, **43**, 084001
Ageron M., et al., 2011, *Nuclear Instruments and Methods in Physics Research A*, **656**, 11
Albert A., et al., 2022, *arXiv e-prints*, p. [arXiv:2212.11876](https://arxiv.org/abs/2212.11876)
Allakhverdyan V. A., et al., 2022, *arXiv e-prints*, p. [arXiv:2210.01650](https://arxiv.org/abs/2210.01650)
Allakhverdyan V. A., et al., 2023, *Phys. Rev. D*, **107**, 042005
Avrorin A. V., et al., 2022, *Journal of Experimental and Theoretical Physics*, **134**, 399

Beasley A. J., Gordon D., Peck A. B., Petrov L., MacMillan D. S., Fomalont E. B., Ma C., 2002, *ApJS*, **141**, 13
Blandford R., Meier D., Readhead A., 2019, *ARA&A*, **57**, 467
Böttcher M., 2019, *Galaxies*, **7**, 20
Buson S., Tramacere A., Pfeiffer L., Oswald L., Menezes R. d., Azzollini A., Ajello M., 2022, *ApJ*, **933**, L43
Buson S., et al., 2023, *arXiv e-prints*, p. [arXiv:2305.11263](https://arxiv.org/abs/2305.11263)
Fomalont E. B., Petrov L., MacMillan D. S., Gordon D., Ma C., 2003, *AJ*, **126**, 2562
Fusco L. A., Versari F., 2019, in *Proceedings of the 36th International Cosmic Ray Conference (ICRC2019)*. p. 891
Giommi P., Glauch T., Padovani P., Resconi E., Turcati A., Chang Y. L., 2020, *MNRAS*, **497**, 865
Gordon D., et al., 2016, *AJ*, **151**, 154
Hovatta T., et al., 2021, *A&A*, **650**, A83
IceCube Collaboration 2020, All-Sky Point-Source IceCube Data: Years 2012-2015, [doi:10.21234/EXM3-TM26](https://doi.org/10.21234/EXM3-TM26), <https://icecube.wisc.edu/science/data/7yrPS>
IceCube Collaboration 2021a, GRB Coordinates Network, **29493**, 1
IceCube Collaboration 2021b, GRB Coordinates Network, **30651**, 1
IceCube Collaboration 2021c, GRB Coordinates Network, **30872**, 1
IceCube Collaboration 2022a, GRB Coordinates Network, **31560**, 1
IceCube Collaboration 2022b, GRB Coordinates Network, **31681**, 1
IceCube Collaboration 2022c, GRB Coordinates Network, **31709**, 1
IceCube Collaboration 2022d, GRB Coordinates Network, **31971**, 1
IceCube Collaboration 2022e, GRB Coordinates Network, **32049**, 1
IceCube Collaboration 2022f, GRB Coordinates Network, **33094**, 1
IceCube Collaboration 2022g, GRB Coordinates Network, **33117**, 1
IceCube Collaboration 2022h, GRB Coordinates Network, **33122**, 1
IceCube Collaboration 2022i, GRB Coordinates Network, **33127**, 1
IceCube Collaboration et al., 2021, *arXiv e-prints*, p. [arXiv:2101.09836](https://arxiv.org/abs/2101.09836)
Kadler M., et al., 2016, *Nature Physics*, **12**, 807
Kalashev O. E., Kivokurtseva P., Troitsky S., 2022, *arXiv e-prints*, p. [arXiv:2212.03151](https://arxiv.org/abs/2212.03151)
Kovalev Y. Y., Petrov L., Fomalont E. B., Gordon D., 2007, *AJ*, **133**, 1236
Kovalev Y. Y., Plavin A. V., Troitsky S. V., 2022, *ApJ*, **940**, L41
Kun E., Bartos I., Becker Tjus J., Biermann P. L., Franckowiak A., Halzen F., 2022, *ApJ*, **934**, 180
Lagunas C., Ashida Y., Sharma A., Thomas H., 2021, *arXiv e-prints*, p. [arXiv:2107.08670](https://arxiv.org/abs/2107.08670)
Mészáros P., 2017, *Annual Review of Nuclear and Particle Science*, **67**, 45
Neronov A., Semikoz D., 2021, *JETP Lett.*, **113**, 69
Neronov A., Savchenko D., Semikoz D. V., 2023, *arXiv e-prints*, p. [arXiv:2306.09018](https://arxiv.org/abs/2306.09018)
Petrov L., 2011, *AJ*, **142**, 105
Petrov L., 2012, *MNRAS*, **419**, 1097
Petrov L., 2013, *AJ*, **146**, 5
Petrov L., 2021, *AJ*, **161**, 14
Petrov L., Kovalev Y. Y., Fomalont E., Gordon D., 2005, *AJ*, **129**, 1163
Petrov L., Kovalev Y. Y., Fomalont E. B., Gordon D., 2006, *AJ*, **131**, 1872
Petrov L., Kovalev Y. Y., Fomalont E. B., Gordon D., 2008, *AJ*, **136**, 580
Petrov L., Gordon D., Gipson J., MacMillan D., Ma C., Fomalont E., Walker R. C., Carabajal C., 2009, *Journal of Geodesy*, **83**, 859
Petrov L., Kovalev Y. Y., Fomalont E. B., Gordon D., 2011a, *AJ*, **142**, 35
Petrov L., Phillips C., Bertarini A., Murphy T., Sadler E. M., 2011b, *MNRAS*, **414**, 2528
Petrov L., de Witt A., Sadler E. M., Phillips C., Horiuchi S., 2019, *MNRAS*, **485**, 88
Piner B. G., et al., 2012, *ApJ*, **758**, 84
Plavin A., Kovalev Y. Y., Kovalev Y. A., Troitsky S., 2020, *ApJ*, **894**, 101
Plavin A. V., Kovalev Y. Y., Kovalev Y. A., Troitsky S. V., 2021, *ApJ*, **908**, 157
Plavin A., Kovalev Y. Y., Kovalev Y. A., Troitsky S., 2022, in *37th International Cosmic Ray Conference*. p. 967 ([arXiv:2112.09053](https://arxiv.org/abs/2112.09053)), [doi:10.22323/1.395.0967](https://doi.org/10.22323/1.395.0967)
Plavin A. V., Burenin R. A., Kovalev Y. Y., Lutovinov A. A., Starobinsky A. A., Troitsky S. V., Zakharov E. I., 2023a, *arXiv e-prints*, p. [arXiv:2306.00960](https://arxiv.org/abs/2306.00960)

- Plavin A. V., Kovalev Y. Y., Kovalev Y. A., Troitsky S. V., 2023b, *MNRAS*, **523**, 1799
- Pushkarev A. B., Kovalev Y. Y., 2012, *A&A*, **544**, A34
- Reusch S., et al., 2022, *Phys. Rev. Lett.*, **128**, 221101
- Rodrigues X., Garrappa S., Gao S., Paliya V. S., Franckowiak A., Winter W., 2021, *ApJ*, **912**, 54
- Sahakyan N., Giommi P., Padovani P., Petropoulou M., Bégué D., Boccardi B., Gasparyan S., 2023, *MNRAS*, **519**, 1396
- Schinzl F. K., Petrov L., Taylor G. B., Mahony E. K., Edwards P. G., Kovalev Y. Y., 2015, *ApJS*, **217**, 4
- Shu F., et al., 2017, *ApJS*, **230**, 13
- Stein R., et al., 2021, *Nature Astron.*, **5**, 510
- Troitsky S. V., 2022, *Physics Uspekhi*, **64**, 1261
- Urry C. M., Padovani P., 1995, *PASP*, **107**, 803
- Zhou B., et al., 2021, *Phys. Rev. D*, **103**, 123018

**SUPPLEMENTARY INFORMATION I:
LIST OF EVENTS**

Table 2 presents the list of 60 high-energy IceCube events used in the present work. Additional information on the events may be found in [Plavin et al. \(2023b\)](#) using event dates (Col. 1) as ID, with the exception of two last events for which we used GCN ([IceCube Collaboration 2022f,h](#)) alert information. Column 2 gives 8-GHz VLBI fluxes of associated blazars (see Supplementary Information II for details; mean if several blazars are associated; zero if no blazar from the RFC complete sample is associated). Column 3 gives the values of flare likelihood L , discussed in Sec. 2.2.

**SUPPLEMENTARY INFORMATION II:
PROCEDURE TO CALCULATE THE ASSOCIATED
BLAZAR FLUX F**

To determine F , one needs to determine which blazar is associated with a particular HE neutrino. We follow the procedure defined by [Plavin et al. \(2020\)](#). Details of the procedure have been fixed in previous works and extensively discussed there. Here we keep the procedure unchanged and describe it for reference.

1. The 90% CL uncertainty in the arrival direction of a HE neutrino is reported by IceCube as

$$\left(\alpha_{-\Delta\alpha_-}^{+\Delta\alpha_+}, \delta_{-\Delta\delta_-}^{+\Delta\delta_+} \right), \quad (1)$$

where α and δ are equatorial coordinates and $\Delta\alpha_{\pm}, \Delta\delta_{\pm}$ are their two-sided uncertainties. Define the 90% CL containment region in the sky enclosed by four quarters of ellipses with corresponding half-axes of $1.3\Delta\alpha_{\pm}, 1.3\Delta\delta_{\pm}$, where the coefficient 1.3 comes from the difference in definitions between one-dimensional and two-dimensional errors.

2. Enlarge the obtained error region by $\Delta_s = 0.45^\circ$ in all directions to compensate for unaccounted systematic errors. The value of Δ_s has been optimized previously, and results of previous works have taken into account the look-elsewhere effect related to this optimization. Here we fix the value of $\Delta_s = 0.45^\circ$ determined previously, do not optimize it and therefore do not need to introduce the corresponding trial correction to our statistical results. Note that the optimal value of 0.5° in [Plavin et al. \(2020\)](#) was found with a computer code having a minor inconsistency ([Plavin et al. 2023b](#)), and the correct value of 0.45° applies to both the original ([Plavin et al. 2020](#)) and updated ([Plavin et al. 2023b](#)) samples. Note also that [Abbasi et al. \(2023b\)](#) revealed that, at least for recent events, the 90% CL uncertainties reported in the form (1) by IceCube do not have the meaning of one-dimensional statistical errors, but indicate the corners of a rectangular region in the sky containing the 90% uncertainty area, hence the multiplication by 1.3 is not needed. [Plavin et al. \(2023a\)](#) demonstrated that without the multiplication, the optimal value of Δ_s becomes equal to 0.78, without any change in results with respect to the previously defined procedure. In the present work, we use the established procedure of multiplying by 1.3 and adding $\Delta_s = 0.45^\circ$.

3. A source from the complete VLBI-selected RFC sample discussed in Sec. 2.3, which falls within the enlarged error contour described above, is considered as associated with the corresponding HE neutrino. If one source is associated, then F equals to its 8-GHz VLBI flux density from the RFC catalog. In case there are several sources associated with one HE neutrino, F equals to the geometric mean of their flux densities. If no blazar is associated, then $F = 0$. Note that the RFC catalog gives the time-averaged historical flux densities and hence does not directly trace possible flares at the HE neutrino arrival time.

Event date	VLBI flux, Jy	L
2011-06-10	0.	0.
2011-07-14	1.358	0.
2011-09-30	4.034	0.67
2012-03-01	0.	0.
2012-05-15	0.916	1.1
2012-05-23	0.821	0.
2012-08-07	0.	0.
2012-09-22	0.	0.
2012-10-11	0.225	1.28
2012-10-26	0.	0.
2013-06-27	0.337	0.
2013-10-14	0.628	0.
2013-10-23	0.176	0.
2013-12-04	0.236	1.15
2014-01-08	0.179	0.68
2014-01-09	0.	0.
2014-01-22	0.	0.
2014-02-03	0.519	0.
2014-06-09	0.	0.
2014-06-11	0.	0.
2014-09-23	0.	0.
2015-01-27	0.	0.
2015-05-15	0.	0.
2015-07-14	0.	0.
2015-08-12	1.532	1.45
2015-08-31	1.627	0.
2015-09-04	0.341	0.
2015-09-23	0.	0.
2015-09-26	15.383	0.
2015-11-14	0.636	0.
2015-11-22	0.	0.
2016-01-28	0.865	0.
2016-03-31	0.205	0.
2016-05-10	0.	0.
2016-07-31	0.	0.
2016-08-06	0.	0.
2016-12-10	0.	0.97
2017-03-21	0.429	0.
2017-09-22	0.447	0.
2017-11-06	0.211	0.96
2018-09-08	0.258	1.31
2018-10-23	0.	0.
2019-05-03	0.	0.
2019-07-30	0.53	0.
2020-06-15	0.	0.
2020-09-26	0.	0.
2020-10-07	0.	0.
2020-11-14	0.	0.
2020-11-30	0.476	0.9
2020-12-09	0.	0.
2021-02-10	0.	0.
2021-08-11	0.194	0.
2021-09-22	0.	0.
2022-02-05	4.034	1.52
2022-03-03	0.71	0.92
2022-03-06	0.	0.
2022-04-25	0.168	0.
2022-05-13	0.221	0.
2022-12-23	0.	0.
2022-12-29	0.232	0.

Table 2. Data used in the present study (see the text for details).

SUPPLEMENTARY INFORMATION III: TEST STATISTICS FOR CORRELATIONS

III.1. The flux-ratio f statistics

The flux-ratio test is a simple “yes or no” test motivated for the present study because a relation between the likelihood value L and the corresponding flare flux is not known. It measures the deviation from a random expectation in fluxes of blazars associated with events with nonzero L , compared to those with $L = 0$. We define the corresponding test statistics f below and use Monte-Carlo simulations, Sec. 3, to relate the value of τ to the significance of correlations, see Fig. 4.

Consider the set $\{F_i\}$ of $n = 60$ mean blazar fluxes and the set $\{L_i\}$ of corresponding flare likelihoods. The flux ratio statistics is determined as the ratio of mean fluxes,

$$f = \frac{\langle F_{i: L_i \neq 0} \rangle}{\langle F_{i: L_i = 0} \rangle}.$$

Like elsewhere in the paper, the mean flux is understood as the geometric mean.

III.2. The Spearman ρ statistics

The Spearman rank test is a standard tool for estimation of the significance of correlations between two sets of data. For reference, we present here the definition of the corresponding test statistics ρ . We use Monte-Carlo simulations, Sec. 3, to relate the value of ρ to the significance of correlations, see Fig. 3 in Sec. 3.

Consider the set $\{F_i\}$ of $n = 60$ mean blazar fluxes and the set $\{L_i\}$ of corresponding flare likelihoods. For each L_i , denote as $r_{L,i}$ its rank (the number it would have in an ordered list of the same values). Some of values may repeat (e.g., a large number of zero values); the ranks of corresponding elements are then replaced by their average, so that all equal values in the list have equal ranks (possibly non-integer). Let $m_{L,j}$ be the multiplicity of each value of $r_{L,i}$, where j runs over non-equal values of ranks in $\{L_i\}$.

The list $\{F_i\}$ also has equal elements, including a number of zero elements and those coming from two events associated with the same blazar, PKS 1741–038. Let $r_{F,i}$ and $m_{F,k}$ be the ranks and multiplicities defined in a similar way, where k runs over non-equal values of ranks in $\{F_i\}$. The test statistics is then

$$\rho = \frac{\frac{1}{6}(n^3 - n) - T_F - T_L - \sum_i (r_{F,i} - r_{L,i})^2}{\sqrt{\left(\frac{1}{6}(n^3 - n) - 2T_F\right) \left(\frac{1}{6}(n^3 - n) - 2T_L\right)}},$$

where the corrections for ties are

$$T_F = \frac{1}{12} \sum_k (m_{F,k}^3 - m_{F,k}),$$

$$T_L = \frac{1}{12} \sum_j (m_{L,j}^3 - m_{L,j}).$$

III.3. The Kendall τ statistics

The Kendall rank correlation coefficient is another frequently used tool for estimation of the significance of correlations between two sets of data. For reference, we present here the definition of the corresponding test statistics τ . We use Monte-Carlo simulations, Sec. 3, to relate the value of τ to the significance of correlations, see Fig. 5.

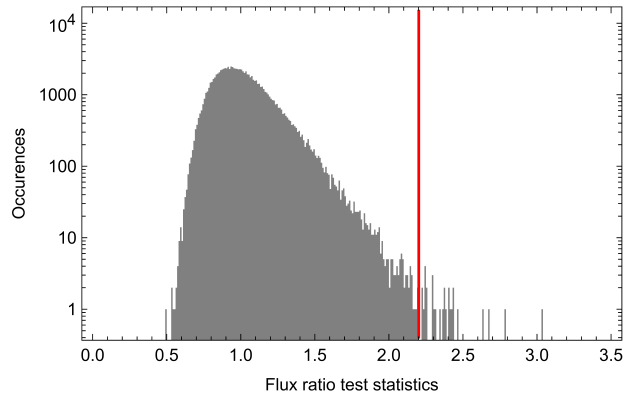


Figure 4. Distribution of the flux-ratio test statistics f for 10^5 randomized data sets (gray histogram) and the value of f_0 for the real data (vertical red line). Only 30 of 10^5 simulated sets have $f \geq f_0$.

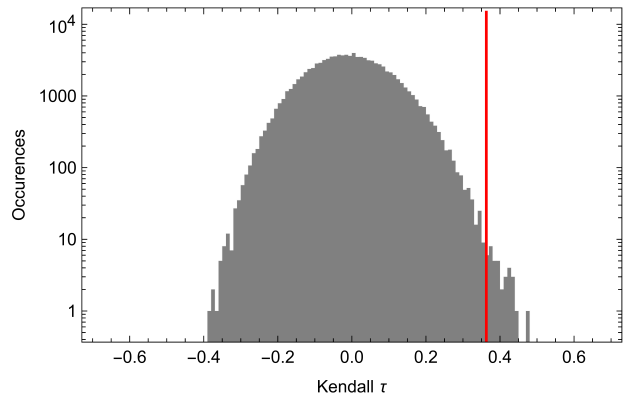


Figure 5. Distribution of Kendall test statistics τ for 10^5 randomized data sets (gray histogram) and the value of τ_0 for the real data (vertical red line). Only 35 of 10^5 simulated sets have $\tau \geq \tau_0$.

Consider the set $\{\Pi_i\}$ of $n = 60$ pairs $\Pi_i = (F_i, L_i)$ of mean blazar fluxes F_i and corresponding flare likelihoods L_i . Construct various pairs of pairs (Π_i, Π_j) . A pair of pairs is called *concordant* if either both $F_i < F_j$ and $L_i < L_j$, or both $F_i > F_j$ and $L_i > L_j$. It is called *discordant* if either $F_i < F_j$ but $L_i > L_j$, or $F_i > F_j$ but $L_i < L_j$. The test statistics is defined as

$$\tau = \frac{n_c - n_d}{\sqrt{(n_c + n_d + n_F)(n_c + n_d + n_L)}},$$

where n_c is the number of concordant pairs of pairs, n_d is the number of discordant ones, n_F and n_L are the numbers of ties, or groups of repeated elements, in the $\{F_i\}$ and $\{L_i\}$ sets, correspondingly.

This paper has been typeset from a $\text{\TeX}/\text{\LaTeX}$ file prepared by the author.